Front. Optoelectron. 2012, 5(3): 239–247
DOI 10.1007/s12200-012-0277-7

REVIEW ARTICLE

Optically pumped semiconductor nanowire lasers

Yaoguang MA, Limin TONG (✉)

State Key Laboratory of Modern Optical Instrumentation, Department of Optical Engineering, Zhejiang University, Hangzhou 310027, China

Abstract This paper reviews our recent work on fabrication, optical characterization and lasing application of semiconductor nanowires, with brief introduction of related work from many other groups.

Keywords semiconductor nanowire, nanowire laser, optical pump, microfiber

1 Introduction

The famous talk "There's plenty of room at the bottom" given by Richard Feynman at the annual meeting of the American Physical Society (APS) in 1959 [1] have promoted "miniaturization" a long-term theme for modern technologies. Thereafter, similar to reducing dimensions of electronic devices, miniaturization of photonic devices including lasers has been attracting increasing interests for higher flexibilities, better performances and higher-density integration. The combination of nanotechnology and lasers physics conceived the idea of nanowire lasers, which generally refer to miniaturized lasers composed by one-dimensional (1D) nanostructures, such as nanowires and nanoribbons [2].

Usually, semiconductor nanowires for laser applications are fabricated by bottom-up chemical growth, such as vapor-liquid-solid (VLS) method [3], with typical diameters of tens of hundreds of nanometers and lengths of several to hundreds of micrometers [4]. These 1D active nanowires are usually direct bandgap material with large refractive index and widely available bandgaps, which make them ideal candidates for nanowire lasers covering a broad spectral range. Also, the 1D geometry and high uniformity make the nanowires excellent optical waveguides for direction and recirculation of light on micro/nanometer scale.

Compared to other types of nanoscale lasers, such as microdisk lasers and vertical cavity surface emitting laser (VCSEL), nanowire lasers are waveguide lasers that benefit far more than the capability of dense integration. For example, the output light of a nanowire waveguide could be directly coupled into both photonic and plasmonic nanostructures with high efficiency [5,6]. And the light recirculation in the subwavelength-diameter waveguide offers opportunities for enhancing interaction with surrounding media, as well as for modifying the output of the laser itself. All these merits of nanowire lasers make them fascinating building blocks for future micro/nanophotonic devices and circuits.

In this review article, we first introduce the synthesis method of semiconductor nanowires and their optical properties. After a brief historical review of semiconductor nanowire lasers of different structures, we then present single semiconductor nanowire lasers and microfiber coupled semiconductor nanowire lasers, with the most recent progresses in realizing single mode lasing in semiconductor nanowires. Finally, we give a breif summary and outlook of semiconductor nanowire lasers.

2 Fabrication and characterization of semiconductor nanowires

Typically, there are two methods for fabricating semiconductor nanowires: the bottom-up vapor deposition technique such as VLS method and the top-down lithography approach. The vapor deposition technique surpasses the lithography by allowing good surface quality and low cost. First proposed in 1960s [7], the VLS method has been greatly improved for nanowire growth over the past two decades [3,8–10]. A typical VLS process includes the formation of liquid droplet, alloying, nucleation, and growth to single-crystalline nanowires, as shown in Fig. 1(a). A typical setup for nanowire growth is schematically illustrated in Fig. 1(b). A clean and defect-free substrate is first deposited with a thin layer of metal (usually gold) as catalyst. Second, as-prepared substrate and the target material are heated in a reaction tube. The metal film agglomerates into liquid droplets when

Received May 2, 2012; accepted June 4, 2012

E-mail: phytong@zju.edu.cn

contacted with the sublimed reactants due to a reduced melting temperature of the metal-semiconductor alloy. These as-formed liquid alloys will dissolve the reactants continually and initiate the subsequent growth from supersaturated droplets, leading to a precipitation and crystallization of the target material onto the substrate.

Recently, we demonstrated a facile thermal evaporation method based on the VLS mechanism [11,12], and realized the spatial bandgap engineering in single semiconductor alloy nanowires. Along the length of these achieved nanowires, the composition was continuously tuned, enabling the corresponding bandgap (light emission wavelength) being modulated to cover the entire visible range, as shown in Figs. 1(c) and 1(d). It is noticed that, in spite of the lattice and composition (crystal lattice) transition along the length, the nanowire exhibited high quality crystallization.

3 Optical properties of nanowires

3.1 Endface reflectivity of a nanowire

The endface reflectivity is one of the most important parameters for a nanowire laser that relies on Fabry-Pérot (F-P) cavity formed by the endface reflection, which determins the cavity quality factor Q and thus the lasing threshold. Unlike in bulk components that the reflectivity can be simply obtained by the Fresnel formula [2], the endface reflectivity of a nanowire is largely affected by the diffraction of the subwavelength endface.

Generally, endface reflectivity of a nanowire mainly depends on the mode confinement and refractive-index contrast of the nanowire. Usually, better confinement and high refractive-index contrast lead to higher reflectivity. Maslov and Ning [13] have calculated light-frequency-dependent reflection coefficient of the first three guided modes of a nanowire with dielectric constant of 6, show that the endface reflectivity increases with the increasing of light frequency and the reflectivity tends to reach a certain value when the field is confined within the nanowire, as shown in Fig. 2(a). We have also obtained the refractive-index-dependent endface reflectivity of nanowires with some typical diameters and wavelengths in Fig. 2(b).

3.2 Coupling between closely contacted parallel nanowires

Evanescent coupling between two parallel nanowires is of

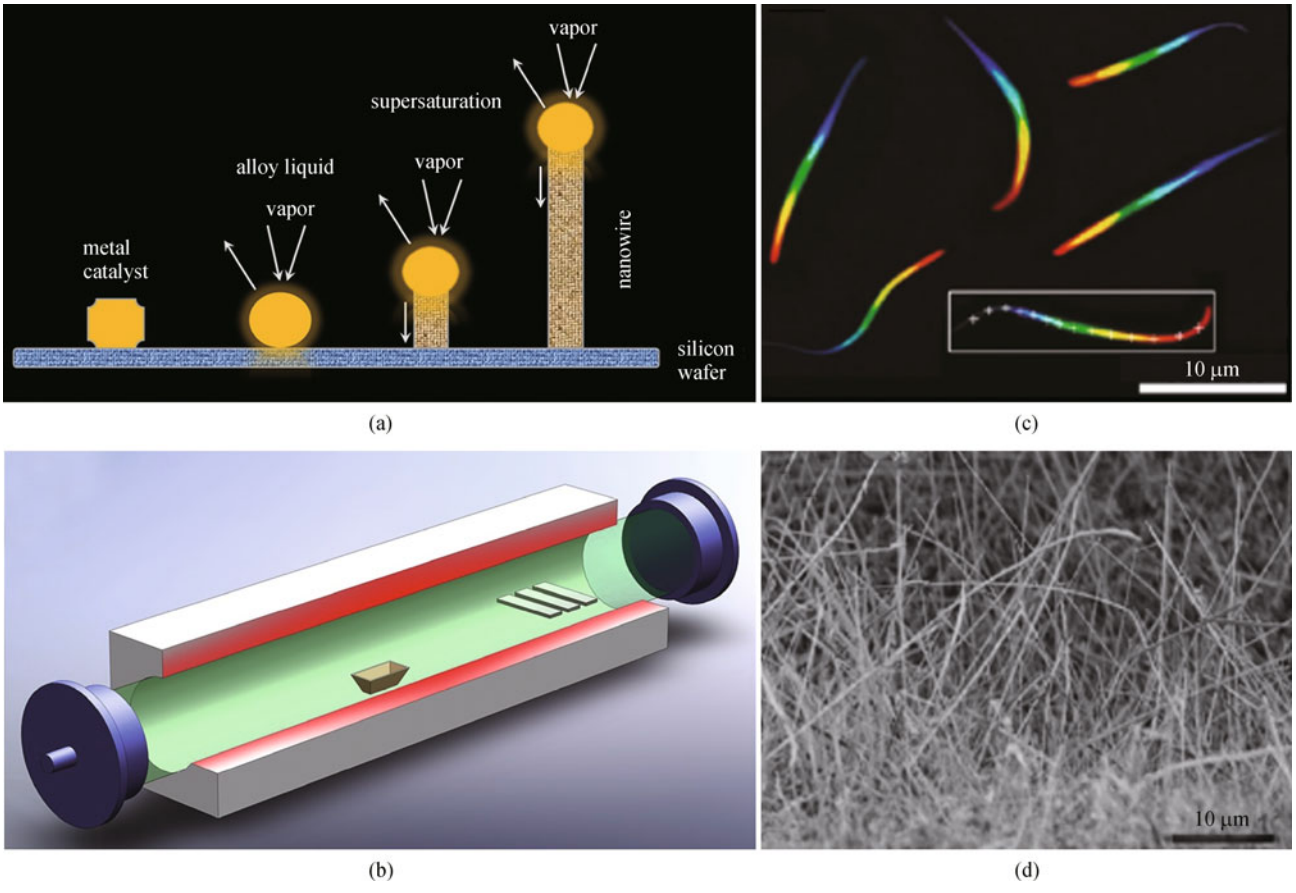

Fig. 1 Semiconductor nanowire growth: schematic illustrations of (a) VLS nanowire growth mechanism; (b) typical setup for VLS growth; (c) optical microscope image of bandgap-modulated ZnCdSSe nanowires under 355 nm light illuminations [12]; (d) sideview SEM image of as-grown ZnCdSSe nanowires [12]

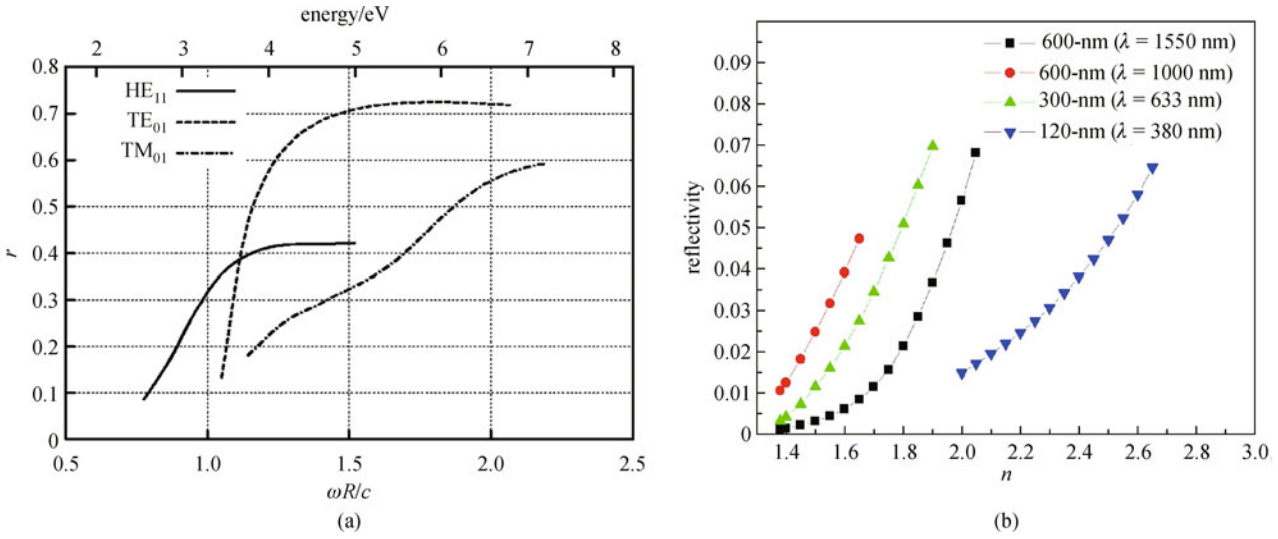

Fig. 2 Endface reflectivity of waveguiding nanowires. (a) Reflection coefficient for the first three guided modes of a nanowire with dielectric constant of 6 (energy for R = 60 nm) [13]; (b) refractive-index-dependent endface reflectivity of nanowires with some typical diameters and wavelengths [14]

special importance for applications, such as near-field-coupling-based functional components and in/out coupling with external optical systems. Usually, weak evanescent coupling between adjacent waveguides can be described by the perturbation theory [15]. However, for closely contacted nanowires that have strong evanescent coupling, a more accurate approach is solving Maxwell's equations numerically [16]. For reference, Fig. 3(a) shows a three-dimensional (3D) finite element method (FEM) simulation of strong coupling between two 160-nm-diameter nanowires with refractive index of 2.0.

Based on finite-difference time-domain (FDTD) calculation, Huang et al. [16] obtained the coupling efficiency (η) between two parallel nanowires, which showed that η was always considerably higher than zero (e.g., η_{min}~34% for two 350 nm diameter silica nanowires) and lower than 100% (e.g., $\eta_{max} > 96\%$ for 350 nm diameter nanowires with z polarization) due to the strong evanescent coupling. At a given wavelength, coupling between two different nanowires was direction dependent: coupling from a high-effective-index nanowire to a low-effective-index nanowire exhibited higher η_{max} (the maximum coupling efficiency), lower η_{min} (the minimum coupling efficiency) and shorter coupling length than those with opposite direction, as shown in Fig. 3(b).

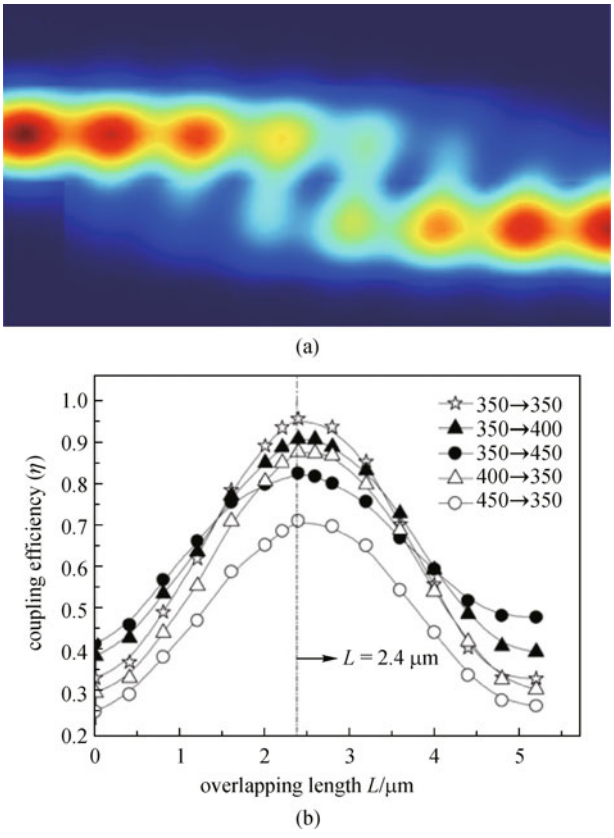

Fig. 3 Coupling between closely contacted parallel nanowires. (a) 3D FEM simulation of light coupling between two 160 nm diameter nanowires with refractive index of 2.0; (b) couping efficiency between two nanowires with different wavelengths, couping lengths and separation distances [16]

3.3 Substrate induced optical effects

In most cases, a freestanding semiconductor nanowire needs supporting substrates for device applications. The effects induced by the substrate, such as mode transformation and leakage, have been investigated by several groups [17,18]. There are mainly two factors responsible for these

effects. Firstly, imperfections on the surface of the substrate will cause scattering loss of the guiding modes by evanescent coupling [17]. Usually, the thinner the nanowire is, the larger the scattering will loss. The fractional energy propagated inside the substrate is also depended on the polarization, leading to a polarization-dependent leakage loss [19]. Secondly, when the index-contrast is not high enough, the appearance of the substrate will lead to the leakage of the guiding mode previously propagated in the nanowire, resulting in no supporting mode in the overall nanowire-substrate system, as shown in Fig. 4(b) [15]. It is worth to note that this substrate-induced leakage has been used for developing compact nanowire/nanofiber short-pass filters [18].

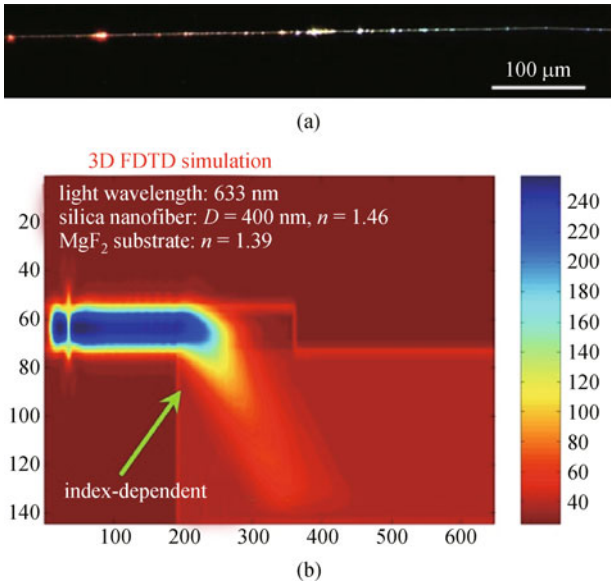

Fig. 4 Substrate induced effects in semiconductor nanowires. (a) Optical short pass filter based on substrate induced leakage [18]; (b) 3D FDTD simulation of substrate induced leakage

4 Optically pumped nanowire lasers

4.1 Single nanowire lasers

In 2001, Huang et al. reported room-temperature laser emission from ZnO nanowires [20], which has attracted considerable attentions of the nanowire lasing. So far, optically pumped coherent laser emission has been observed from a number of nanocavities of binary semiconductors, including ZnO (λ ~ 385 nm) single nanowires/ nanoribbons [21] and combs [22], ZnS (~337 nm) nanoribbons [23], GaN (~375 nm) single nanowires and ring resonators [24,25], CdS (~500 nm) single nanowires and ring resonators [19,26], and CdSe single nanowires [27], GaSb (~1550 nm) nanowires [28].

Generally, a semiconductor nanowire with large refractive-index-contrast against the surrounding medium can be operated as an F-P cavity for lasing resonance. However, if the nanowire diameter is too small (e.g., < 100 nm), the optical resonance will suffer very weak reflection and significant leakage (to the substrate) loss, which may prevent the lasing activity in these nanowires.

Figure 5 shows optical characterization of a 12.2 μm long 250 nm diameter ZnO semiconductor nanowire laser. When under pumping, the luminescence of semiconductor nanowire will first increase in a linear way (see Figs. 5(c) and 5(d)), with the excitation intensity which strongly indicates spontaneous emission dominates the photoluminescence (PL). When the excitation intensity is enhanced, one of the resonant modes sharpens considerably and gains height as the nanowires reaches the amplified spontaneous emission (ASE) state [29]. Furthermore, the output power of this mode will exhibit a superlinear increase with pump intensity as shown in Fig. 5(d) clearly, which is expected as the laser threshold is approached. After a further increase of the excitation intensity, this mode and other neighboring modes will form dominant lasing modes. The intensity of these lasing modes is orders of magnitude greater than the spontaneous emission background, and the output power will again depend linearly on excitation intensity and is concentrated in a narrow emission range.

4.2 Microfiber coupled semiconductor nanowire lasers

The progress in fabrication and applications of low-loss micro-/nanofibers has led to high quality factor micro-resonators in the form of loop or knot structures. Compared with semiconductor nanowire cavities with relatively low Q factors, the Q factor of a microfiber knot cavity can go higher than 10^5, suggesting a possible approach to microfiber-nanowire-integrated lasing devices with low thresholds.

In 2009, Yang et al. [30] reported a hybrid lasing structure fabricate by attaching semiconductor nanowires to a silica microfiber knot resonator. As shown in Fig. 6, pumped by frequency-tripled Nd:YAG laser pulses (355 nm, 6 ns, and 10 Hz), the PL from the nanowire is coupled into the knot resonator and circulated as guiding modes of the microfiber. When the cavity round-trip gain surpasses the round-trip loss, lasing oscillation occurs in the knot resonator. Sharp peaks in the PL spectra can be seen in Fig. 6, with output power concentrated within a narrow emission range (391 nm < λ < 392 nm).

Another demonstration by Ding et al. [31] is a microfiber-nanowire hybrid structure multicolor laser. As shown in Fig. 7(a), CdSe, CdS and ZnO nanowires with different bandgaps are attached onto a microfiber. The pumping light launched into the microfiber excited the nanowires evanescently, with red, green and ultraviolet PL generated from CdSe, CdS and ZnO nanowires (see Fig. 7(b)), respectively. Based on the F-P resonance generated by the endface reflection of the individual

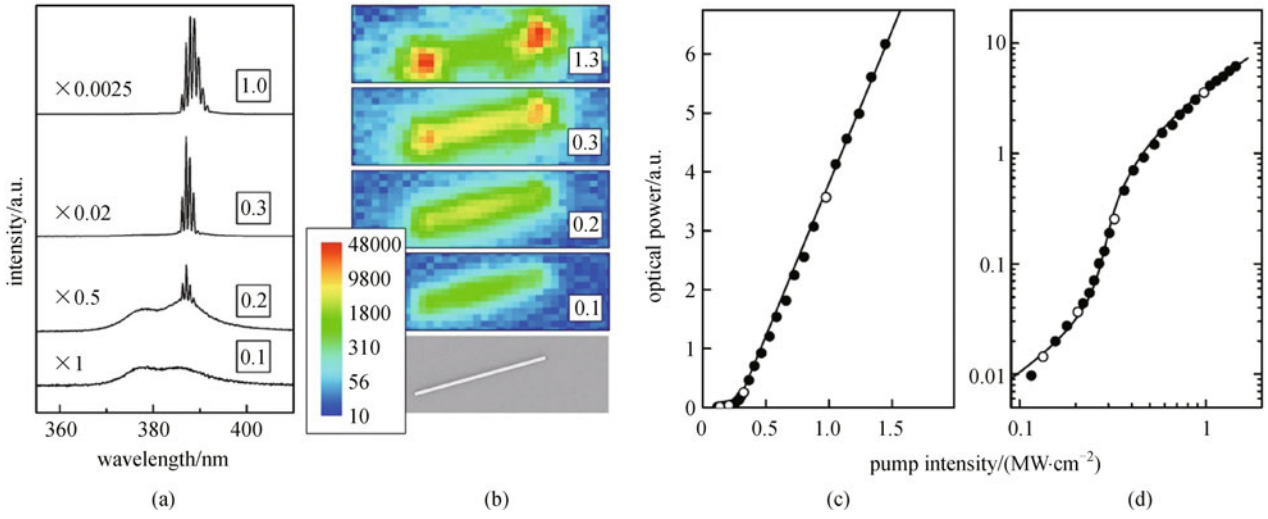

Fig. 5 Optical characterization of a 12.2 μm long 250 nm diameter ZnO semiconductor nanowire laser [29]. (a) Output spectra versus pump intensity of a ZnO nanowire laser; (b) SEM image and CCD images for the same nanowire as in (a) under different pump intensities; (c) pump intensity dependence of the total output power (circles) for the same nanowire; (d) same data and fit on log-log scale

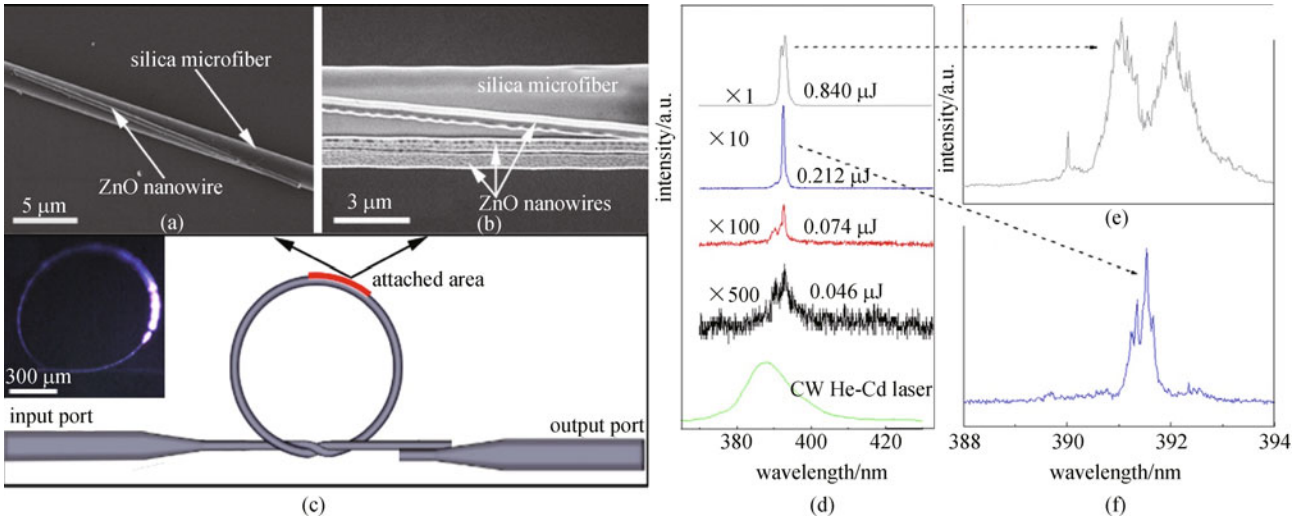

Fig. 6 Microfiber-knot-resonator coupled semiconductor nanowire laser [30]. (a) SEM image of attached area of 25 μm long 350 nm diameter ZnO nanowire and 780 μm diameter microfiber knot assembled with 1.8 μm diameter silica microfiber; (b) SEM image of attached area of three ZnO nanowires and 728 μm diameter silica microfiber knot assembled with 3.5 μm diameter silica microfiber, the diameters of ZnO nanowires are 500, 480, and 600 nm, respectively; (c) schematic diagram of the structure of hybrid laser. Inset: CCD image of the hybrid structure pumped by 355 nm wavelength laser pulses; (d) output spectra versus pump energy of hybrid structure (same structure shown in Fig. 1(a)); (e) and (f) close-up views of two laser spectra in (d)

nanowires, lasing activities around three spectral bands (corresponding to red, green and ultraviolet colors) was observed (Fig. 7(c)).

To combine the high-quality cavity of a ring structure and compatibility with optical fiber system, while miniaturize the overall size of a semiconductor nanowire laser, Ma et al. [19] reported a pigtailed CdS nanoribbon ring laser with convenient connection to a standard optical fiber by out-coupling of the laser from the pigtail to a microfiber. As shown in Fig. 8, a 600 nm wide and 330 nm thick CdS nanoribbon ring cavity was assembled via micromanipulations under an optical microscope by circularly folding of a nanoribbon in a side-by-side geometry with a pigtail structure. When pumped by light from a supercontinuum source (1 ns pulse duration, 24 kHz repetition frequency), lasing emission output from the optical fiber was obtained.

The spectrum of the out coupled emission was shown in Fig. 8(c), the lasing peaks centered at 523.5 nm has a full width at half maximum (FWHM) of about 0.27 nm, with a

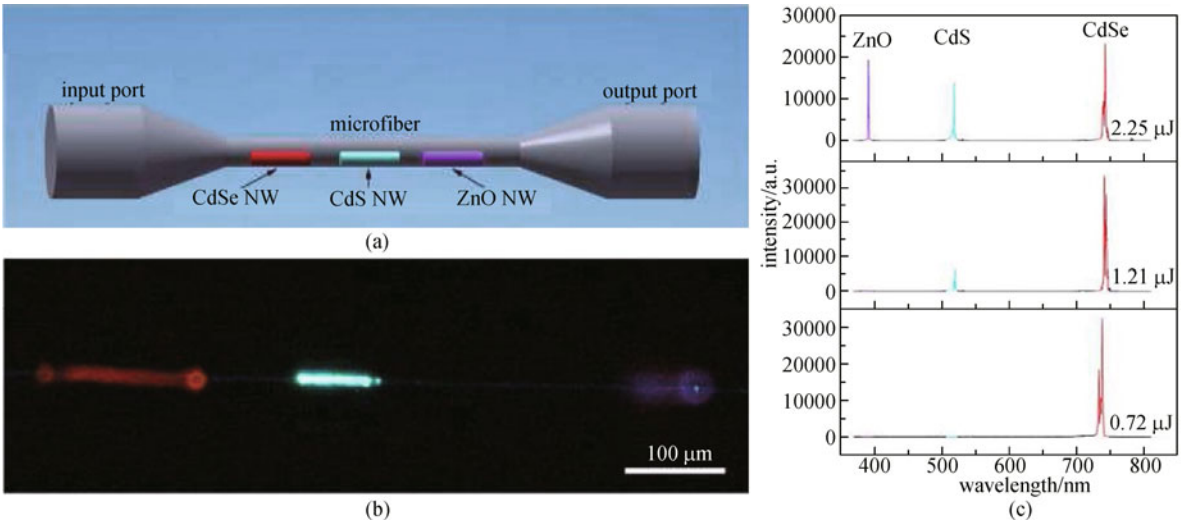

Fig. 7 Microfiber coupled multicolor semiconductor nanowire laser [31]. (a) Schematic configuration of the red-green-ultraviolet three-color laser; (b) CCD image of the hybrid structure pumped by 355 nm wavelength laser pulses; (c) emission spectra of the three-color laser shown in (b) under different pump energy

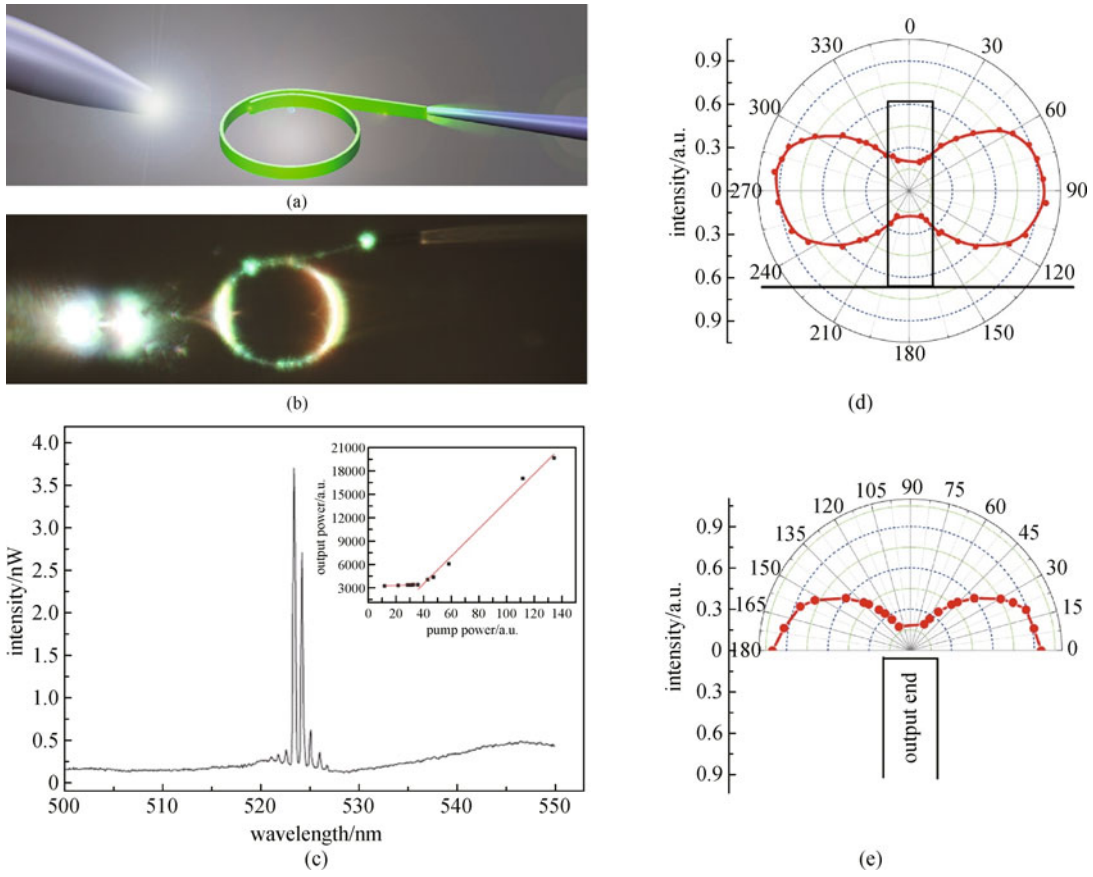

Fig. 8 Pigtailed CdS nanoribbon ring laser [19]. (a) Schematic of structure of nanoribbon ring laser system; (b) optical micrographs of 20 μm diameter CdS nanoribbon ring under pumping; scale bar, 10 μm: (the nanoribbon is 600 nm wide and 330 nm thick); (c) collected lasing spectra of the nanoribbon ring. (Inset: integrated emission power versus pump energy of nanoribbon ring laser); (d) and (e) polar plots of the emission intensity from nanoribbon endfacet as a function of polarization angle, (d) front view and (e) side view. Black lines under the square represent the substrate

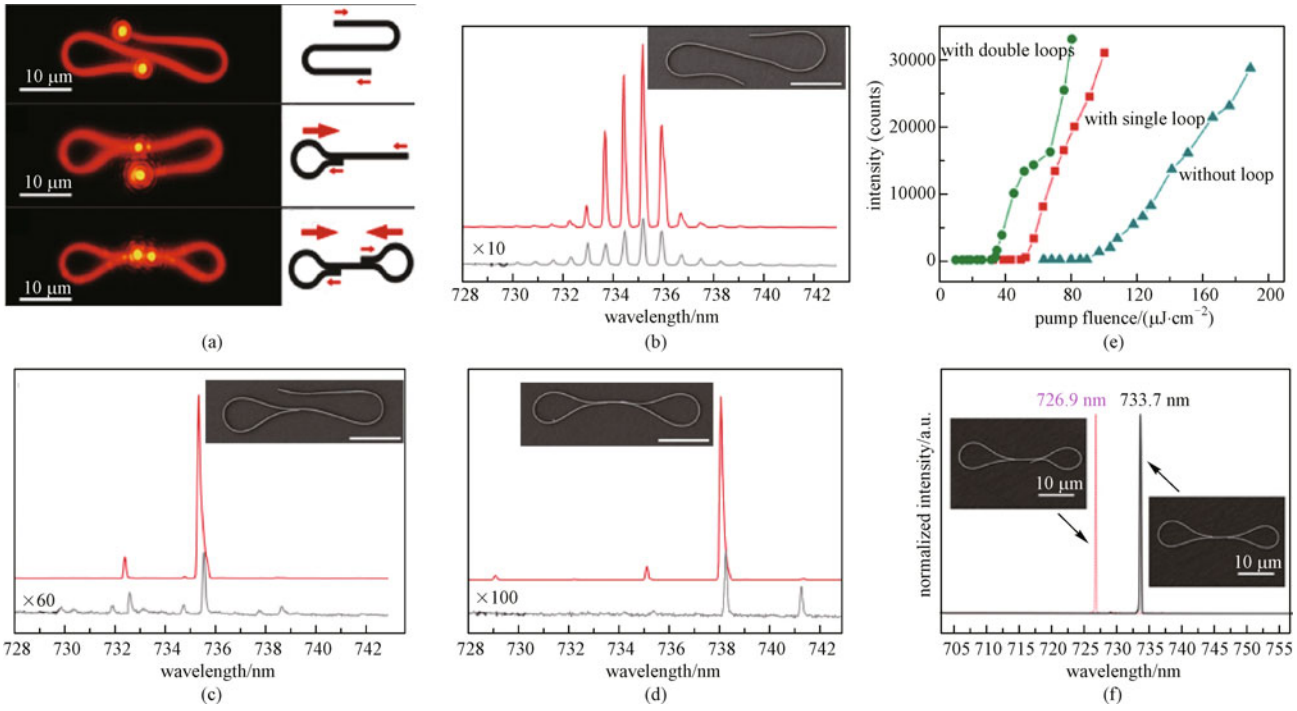

Fig. 9 Single mode single nanowire laser [32]. (a) PL microscope images and schematic diagrams of lasing cavities of single nanowire structures; (b) output lasing spectra of single-nanowire structures without LM; (c) with one LM, and (d) with double LMs. Inset, SEM images of the nanowire cavity corresponding to (b), (c) and (d); (e) emission power vs pump fluence of the excited NW without LM (triangle), with one LM (square), and with double LMs (circle); (f) spectral shift of the lasing peak from 733.7 to 726.9 nm by changing the geometry of the loop in a 240 nm diameter 84 μm length CdSe nanowire laser. Inset, SEM images of the original cavity (bottom right) and the changed cavity (up left)

measurable peak power of about 3.7 nW. Also, the rectangular cross-section of the nanoribbon offers the laser output with considerable polarization properties (Figs. 8(d) and 8(e)). The predominant polarization of the output laser emission from the endfacet is parallel to the substrate with a maximum polarization ratio of 5. The orientation-dependent polarization of the laser output is attributed to the accumulation of the polarization-dependent leakage loss of the oscillating modes induced by the substrate.

4.3 Single mode nanowire lasers

Semiconductor nanowire lasers usually exhibit a multi-mode behavior because of the lacking of mode selection capability. One possible route to obtain single-mode lasers is to fabricate distributed-Bragg-reflector (DBR) mirrors on the nanowire, but is difficult to realize experimentally. Another possible scheme is expanding the free space range (FSR) of the multimodes by significantly shortening the optical path of the lasing cavity, until only one mode is left, but this approach will greatly increase the threshold of the laser.

In 2011, Xiao et al. [32] reported a single-nanowire single-mode laser by folding a 200 nm diameter CdSe nanowire into loop mirrors at both sides. As shown in Fig. 9, single-mode laser emission around 738 nm wavelengths is obtained with line width of 0.12 nm and low threshold. The mode selection is realized by the vernier effect of coupled cavities in the folded nanowire. For example, in Fig. 9(c), the coupling of the two cavities offers the lowest common multiple of the FRSs (0.75 and 0.98 nm) of about 2.96 nm (take into account of the width of the lasing peak), which results in selecting only one dominant mode within the lasing range. The highest side mode suppression ratio (SMSR) in double-loop structure nanowire is larger than 10 dB. It is also noticed that, compared to a nanowire relying solely on a endface-reflection F-P cavity, the introduction of loop mirrors and the formation of high-quality coupled cavities significantly reduced the threshold of the nanowire laser as shown in Fig. 9(e). In addition, the loop structure makes it possible to tune the nanowire cavity (Fig. 9(f)), opening an opportunity to realize a tunable single-mode nanowire laser.

Single mode lasing can also be achieved via an alternative approach by coupling two individual nanowires into two coupled cavities. In 2011, Xiao et al. [33] demonstrated single mode lasing in coupled CdSe nanowires. By coupling two 420 nm diameter CdSe nanowires to form an X-structure cavity, single-mode

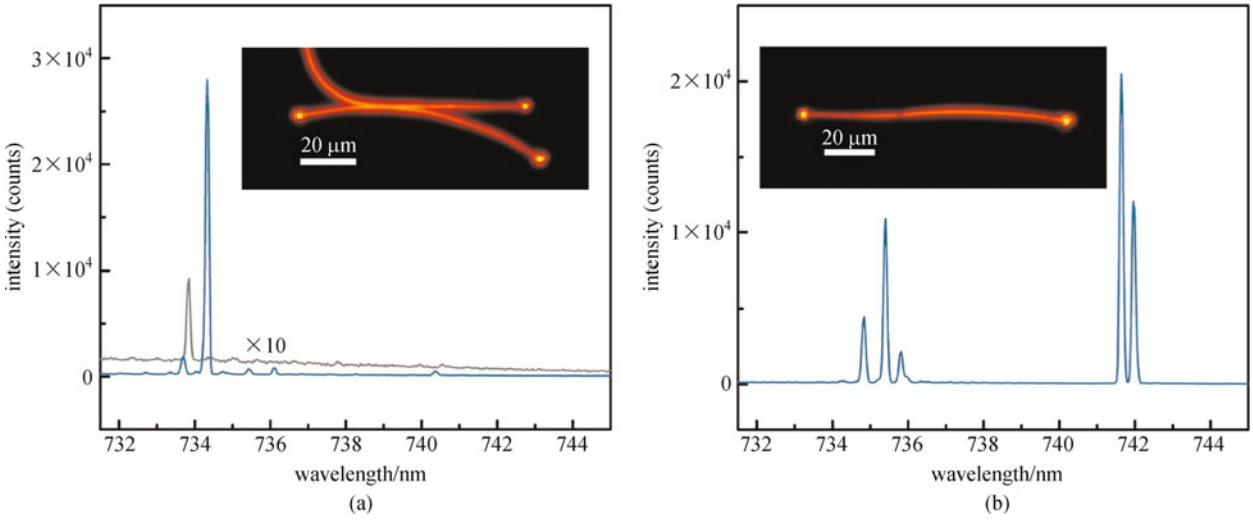

Fig. 10 Single mode laser achieved in coupled nanowires [33]. (a) Single-mode lasing spectra of the X-coupled CdSe nanowires with pumping levels of 151.7 μJ/cm^2 (blue line) and 120.8 μJ/ cm^2 (gray line), respectively. Inset: CCD image of the lasing X-structure; (b) multimode lasing spectra of the individual 89 μm length CdSe nanowires. Inset: CCD image of the lasing nanowire

lasing emission around 734.3 nm is obtained with line width of 0.11 nm and lasing threshold of about 120 μJ/cm^2 (Fig. 10). These results suggest a simple approach to single-mode nanowire lasers.

5 Conclusions and outlook

The past decade has witnessed tremendous exciting progress in the field of semiconductor nanowire lasers. Owning to their advantages such as high mode quality and integratable with nanophotonic circuits, nanowire lasers have been attracting more and more attentions in recent years. However, fundamental and technological issues still remain. First, to be practically useful, a nanowire laser must operate in single mode in most cases. Second, for easy operation and integration with electrically driven chips and devices, the nanowire laser should be able to operate electrically. Third, for optical signal processing, including optical communications and optical computing, the laser should be modulated with high frequency. These concerns have raised great challenges and opportunities for future research on semiconductor nanowire lasers.

References

1. Feynman R P. There's plenty of room at the bottom. IEEE Journal of Microelectromechanical Systems, 1992, 1(1): 60–66
2. Ning C Z. Semiconductor nanolasers. Physica Status Solidi B-Basic Solid State Physics, 2010, 247(4): 774–788
3. Duan X F, Lieber C M. General synthesis of compound semiconductor nanowires. Advanced Materials, 2000, 12(4): 298–302
4. Yan R X, Gargas D, Yang P D. Nanowire photonics. Nature Photonics, 2009, 3(10): 569–576
5. Tong L M, Gattass R R, Ashcom J B, He S L, Lou J Y, Shen M Y, Maxwell I, Mazur E. Subwavelength-diameter silica wires for low-loss optical wave guiding. Nature, 2003, 426(6968): 816–819
6. Guo X, Qiu M, Bao J M, Wiley B J, Yang Q, Zhang X N, Ma Y G, Yu H K, Tong L M. Direct coupling of plasmonic and photonic nanowires for hybrid nanophotonic components and circuits. Nano Letters, 2009, 9(12): 4515–4519
7. Wagner R S, Ellis W C. Vapor-liquid-solid mechanism of single crystal growth. Applied Physics Letters, 1964, 4(5): 89–90
8. Yang P D, Yan H Q, Mao S, Russo R, Johnson J, Saykally R, Morris N, Pham J, He R R, Choi H J. Controlled growth of ZnO nanowires and their optical properties. Advanced Functional Materials, 2002, 12(5): 323–331
9. Xia Y N, Yang P D, Sun Y G, Wu Y Y, Mayers B, Gates B, Yin Y D, Kim F, Yan Y Q. One-dimensional nanostructures: synthesis, characterization, and applications. Advanced Materials, 2003, 15 (5): 353–389
10. Dai Z R, Pan Z W, Wang Z L. Novel nanostructures of functional oxides synthesized by thermal evaporation. Advanced Functional Materials, 2003, 13(1): 9–24
11. Gu F X, Yang Z Y, Yu H K, Xu J Y, Wang P, Tong L M, Pan A L. Spatial bandgap engineering along single alloy nanowires. Journal of the American Chemical Society, 2011, 133(7): 2037–2039
12. Yang Z Y, Xu J Y, Wang P, Zhuang X J, Pan A L, Tong L M. On-nanowire spatial band gap design for white light emission. Nano Letters, 2011, 11(11): 5085–5089
13. Maslov A V, Ning C Z. Reflection of guided modes in a semiconductor nanowire laser. Applied Physics Letters, 2003, 83 (6): 1237–1239
14. Wang S S, Hu Z F, Yu H K, Fang W, Qiu M, Tong L M. Endface reflectivities of optical nanowires. Optics Express, 2009, 17(13):

10881–10886
15. Snyder A W, Love J D. Optical Waveguide Theory. London: Chapman & Hall, 1983
16. Huang K J, Yang S Y, Tong L M. Modeling of evanescent coupling between two parallel optical nanowires. Applied Optics, 2007, 46 (9): 1429–1434
17. Law M, Sirbuly D J, Johnson J C, Goldberger J, Saykally R J, Yang P D. Nanoribbon waveguides for subwavelength photonics integration. Science, 2004, 305(5688): 1269–1273
18. Chen Y, Ma Z, Yang Q, Tong L M. Compact optical short-pass filters based on microfibers. Optics Letters, 2008, 33(21): 2565–2567
19. Ma Y G, Li X Y, Yang Z Y, Yu H K, Wang P, Tong L M. Pigtailed CdS nanoribbon ring laser. Applied Physics Letters, 2010, 97(15): 153122–153123
20. Huang M H, Mao S, Feick H, Yan H Q, Wu Y Y, Kind H, Weber E, Russo R, Yang P D. Room-temperature ultraviolet nanowire nanolasers. Science, 2001, 292(5523): 1897–1899
21. Johnson J C, Yan H Q, Yang P D, Saykally R J. Optical cavity effects in ZnO nanowire lasers and waveguides. Journal of Physical Chemistry B, 2003, 107(34): 8816–8828
22. Yan H Q, He R R, Johnson J, Law M, Saykally R J, Yang P D. Dendritic nanowire ultraviolet laser array. Journal of the American Chemical Society, 2003, 125(16): 4728–4729
23. Zapien J A, Jiang Y, Meng X M, Chen W, Au F C K, Lifshitz Y, Lee S T. Room-temperature single nanoribbon lasers. Applied Physics Letters, 2004, 84(7): 1189–1191
24. Johnson J C, Choi H J, Knutsen K P, Schaller R D, Yang P D, Saykally R J. Single gallium nitride nanowire lasers. Nature Materials, 2002, 1(2): 106–110
25. Pauzauskie P J, Sirbuly D J, Yang P D. Semiconductor nanowire ring resonator laser. Physical Review Letters, 2006, 96(14): 143903
26. Agarwal R, Barrelet C J, Lieber C M. Lasing in single cadmium sulfide nanowire optical cavities. Nano Letters, 2005, 5(5): 917–920
27. Li G, Zhai T, Jiang Y, Bando Y, Golberg D. Enhanced field-emission and red lasing of ordered CdSe nanowire branched arrays. Journal of Physical Chemistry C, 2011, 115(19): 9740–9745
28. Chin A H, Vaddiraju S, Maslov A V, Ning C Z, Sunkara M K, Meyyappan M. Near-infrared semiconductor subwavelength-wire lasers. Applied Physics Letters, 2006, 88(16): 163115–163115-3
29. Zimmler M A, Capasso F, Muller S, Ronning C. Optically pumped nanowire lasers: invited review. Semiconductor Science and Technology, 2010, 25(2): 024001
30. Yang Q, Jiang X S, Guo X, Chen Y, Tong L M. Hybrid structure laser based on semiconductor nanowires and a silica microfiber knot cavity. Applied Physics Letters, 2009, 94(10): 101108
31. Ding Y, Yang Q, Guo X, Wang S S, Gu F X, Fu J, Wan Q, Cheng J P, Tong L M. Nanowires/microfiber hybrid structure multicolor laser. Optics Express, 2009, 17(24): 21813–21818
32. Xiao Y, Meng C, Wang P, Ye Y, Yu H K, Wang S S, Gu F X, Dai L, Tong L M. Single-nanowire single-mode laser. Nano Letters, 2011, 11(3): 1122–1126
33. Xiao Y, Meng C, Wu X Q, Tong L M. Single mode lasing in coupled nanowires. Applied Physics Letters, 2011, 99(2): 023109